Probing DNA Polymerase−DNA Interactions: Examining the Template Strand in Exonuclease Complexes Using 2-Aminopurine Fluorescence and Acrylamide Quenching†

Dina Tleugabulova and Linda J. Reha-Krantz*

Department of Biological Sciences, University of Alberta, Edmonton, Alberta T6G 2E9, Canada

Received February 23, 2007; Revised Manuscript Received April 3, 2007

ABSTRACT: The bacteriophage T4 DNA polymerase forms fluorescent complexes with DNA substrates labeled with 2-aminopurine (2AP) in the template strand; the fluorescence intensity depends on the position of 2AP. When preexonuclease complexes are formed, complexes at the crossroads between polymerase and exonuclease complexes, 2AP in the +1 position in the template strand is fully free of contacts with the adjacent bases as indicated by high fluorescence intensity and a long fluorescence lifetime of about 10.9 ns. Fluorescence intensity decreases for 2AP in the template strand when the primer end is transferred to the exonuclease active center to form exonuclease complexes, which indicates a change in DNA conformation; 2AP can now interact with adjacent bases, which quenches fluorescence emission. Some polymerase-induced base unstacking for 2AP in the template strand in exonuclease complexes is observed but is restricted primarily to the *n* and +1 positions, which indicates that the DNA polymerase holds the template strand in a way that forces base unstacking only in a small region near the primer terminus. A hold on the template strand will help to maintain the correct alignment of the template and primer strands during proofreading. Acrylamide quenches 2AP fluorescence in preexonuclease and in exonuclease complexes formed with DNA labeled with 2AP in the template strand, which indicates that the template strand remains accessible to solvent in both complexes. These studies provide new information about the conformation of the template strand in exonuclease complexes that is not available from structural studies.

DNA replication is a highly dynamic process. During the nucleotide incorporation pathway catalyzed by the bacteriophage T4 DNA polymerase (*1*), correct nucleotides are bound selectively in the polymerase active center by a process that requires at least two conformational changes to assess the accuracy of the newly forming base pair (*2*). Nucleotide selection is followed by formation of the phosphodiester bond, and then the DNA polymerase translocates to be in position to bind the next incoming nucleotide; however, if the wrong nucleotide is incorporated, the proofreading pathway is initiated instead. Proofreading requires extensive conformational changes in the T4 DNA polymerase (*3*, *4*). The conformational changes are needed to separate the primer end from the template strand and to transfer the single-stranded primer end from the polymerase to the exonuclease active center (*5*). After removal of the terminal nucleotide, the trimmed primer end is returned back to the polymerase active center where nucleotide incorporation can resume (*6*).

X-ray crystallographic studies have revealed several informative structures of DNA polymerase complexes with the primer end bound in the polymerase active center, but there is less information about exonuclease complexes. In a structure of an exonuclease complex formed with the RB69 DNA polymerase (*7*), which is highly related to the T4 DNA polymerase (*8*), the DNA substrate has an unnatural overhanging 3′-end. Although this structure clearly shows how the primer end is bound in the exonuclease active center, the absence of an overhanging template strand, an essential feature of replication forks, means that important protein−DNA template strand interactions are missing in this structure. In another structure of an RB69 DNA polymerase exonuclease complex (*4*), the template strand has a short 5′ overhang, but the strand is disordered and, thus, does not provide structural information.

We report here the use of the fluorescence of 2-aminopurine (2AP),[1] an adenine base analogue, to probe the structure of the template strand in exonuclease and preexonuclease complexes formed with the bacteriophage T4 DNA polymerase. 2AP is an excellent fluorophore to probe DNA polymerase−DNA interactions because 2AP can be excited selectively in the presence of DNA and protein, the 2AP nucleotide and 2AP-labeled DNA are substrates, and 2AP fluorescence is a sensitive spectroscopic reporter of DNA conformation. While 2AP as the base, nucleoside, or nucleotide is highly fluorescent, the fluorescence intensity of 2AP is strongly quenched in DNA because of interactions with

† This research was supported by Grant 14300 from the Canadian Institutes of Health Research. L.R.-K. is a Scientist of the Alberta Heritage Foundation for Medical Research.

* To whom correspondence should be addressed. Telephone: 780-492-5383. Fax: 780-492-9234. E-mail: Linda.Reha-Krantz@ualberta.ca.

[1] Abbreviations: 2AP, 2-aminopurine; ssDNA, single-stranded DNA; dsDNA, double-stranded DNA; mmDNA, mismatched DNA; D219A-DNA polymerase, alanine substitution for aspartate 219 producing exonuclease deficiency.

10.1021/bi700380a CCC: $37.00
Published on Web 05/12/2007

adjacent bases (refs *9* and *10* and references cited therein). The fluorescence of 2AP in unbound DNA is characterized typically by four lifetime components that range from about 50 ps to 8 ns or more with the shortest lifetime components (least fluorescent species) predominating (*11*). Even though each lifetime represents the mean of a distribution, lifetimes can be correlated with distinct 2AP conformations (*10*). The shortest lifetime is attributed to a fully stacked state, the longest to the unstacked 2AP, and the intermediates to imperfectly stacked states (*10*−*13*).

Because 2AP fluorescence is modulated by base stacking interactions, 2AP fluorescence intensity can be used as a sensitive reporter of DNA conformation in enzyme complexes if enzyme binding perturbs 2AP interactions with the neighboring bases. For example, when an enzyme such as a methyltransferase flips 2AP out of the DNA helix into the active site pocket, a large increase in fluorescence intensity is observed as expected when 2AP base stacking interactions are relieved. The large enhancement is due to formation of an abundant long lifetime component (>10 ns). For the M.HhaI methyltransferase, the long fluorescence lifetime observed in solution was correlated with 2AP in a flipped-out conformation in crystalline complexes: the very short picosecond lifetime observed for unbound DNA was not detected, and instead the majority (77%) of flipped-out 2AP showed a long lifetime of about 10.9 ns (*10*), which is similar to the free 2AP nucleoside in solution (*9*, *11*).

Time-resolved fluorescence studies of 2AP-labeled DNA in T4 DNA polymerase complexes have also been used to correlate functionally distinct complexes with discrete lifetimes. Large fluorescence enhancements (>30-fold) and long fluorescence lifetimes of about 9−11 ns were detected for exonuclease complexes formed with DNA labeled at the primer end with 2AP (Figure 1A) (*14*). The long lifetimes indicate that the terminal 2AP base is unstacked in the exonuclease active center, which crystal structures show is achieved by intercalation of a phenylalanine residue between the two terminal bases (*4*, *7*).

The template strand also undergoes conformational changes during the proofreading reaction, which we have detected using 2AP fluorescence. A large (>20-fold) increase in fluorescence intensity is detected for 2AP in the +1 position in the template strand for complexes made under conditions that promote formation of preexonuclease complexes: A+T-rich DNA, no dNTPs, and proofreading defective DNA polymerases (*15*−*17*). The large fluorescence enhancement is specific for 2AP in the +1 position of the template strand (*15*), which is the template base for the next incoming nucleotide (Figure 1B); only a small fluorescence enhancement is observed for 2AP at the +2 position. The wild-type T4 DNA polymerase degrades base-paired DNA in the absence of dNTPs (*18*), particularly A+T-rich DNA (*19*, *20*), but preexonuclease complexes are observed with mutant DNA polymerases that cannot readily form stable exonuclease complexes in which the primer end is bound in the exonuclease active center (*17*). Fluorescence enhancement is also observed for 2AP in the template strand when exonuclease complexes are formed in which the primer end is bound in the exonuclease active center, but the enhancement is less than detected for preexonuclease complexes (*15*, *17*).

The different fluorescence intensities of 2AP in the template strand of preexonuclease and exonuclease complexes provide the foundation to further examine the structure of the template strand during the proofreading reaction. Time-resolved fluorescence studies were done with preexonuclease and exonuclease complexes formed with DNA labeled at different positions with 2AP, and fluorescence quenching experiments were done with acrylamide to determine solvent accessibility. Acrylamide is primarily a collisional quencher and therefore to act must be able to reach the fluorophore during the lifetime of the excited state, where contact returns the fluorophore to the ground state without emission of a photon (*21*). For example, if 2AP is located on the surface of a DNA polymerase complex, then efficient acrylamide quenching will be observed, but if 2AP is buried in the complex, then the protein matrix will prevent contact between acrylamide and 2AP, and quenching will not be observed. Both experimental approaches revealed new information about the template strand in exonuclease and preexonuclease complexes formed with the T4 DNA polymerase that is not available from structural studies. Because the T4 DNA polymerase is a model for family B DNA polymerases (*22*), which includes the eukaryotic DNA polymerases δ and ϵ

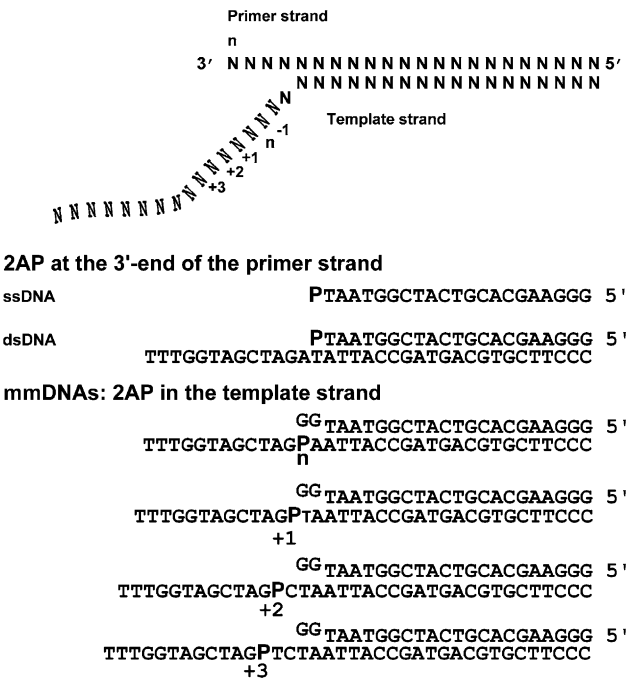

FIGURE 1: DNA substrates used in this study. P indicates the position of 2-aminopurine. The 3′-ends of the template strands are protected by biotin or phosphate groups (not shown) to prevent DNA polymerase binding. (A) Exonuclease complexes: DNA substrates that favor formation of complexes in which the primer end is bound in the exonuclease active center. Structural studies indicate that the 3′-end of the primer strand is buried in a pocket that encompasses the exonuclease active center (*4*, *7*), but there is no information about the single-stranded template strand from the −2 position onward as indicated by the stylized gray letters. (B) Polymerase and preexonuclease complexes: the template/primer is bound in the polymerase active center.

and several viral DNA polymerases (herpes, vaccinia), information learned about proofreading by the T4 DNA polymerase can be extended to these DNA polymerases.

MATERIALS AND METHODS

DNA Polymerases. Expression, purification, and characterization of wild-type T4 DNA polymerase and the exonuclease-deficient D219A-DNA polymerase were described previously (*23*, *24*).

DNA Substrates. The DNA substrates are described in Figure 1. The substrates were prepared as described previously (*15*, *16*, *25*). The 3′ terminus of the template strand of the DNA duplexes was protected from enzyme binding by attachment of a phosphate or biotin group. The 2AP phosphoramidite was purchased from Glen Research. The primer and template strands were annealed in buffer containing HEPES (pH 7.6) and 50 mM NaCl with a 20% excess of the non-2AP-labeled oligomer to ensure complete hybridization of the 2AP-containing strand.

Fluorescence Intensity Experiments. The fluorescence emission spectra were recorded using a Photon Technology International scanning spectrofluorometer (PTI). All 2AP solutions (2AP as the free base, in DNA, and in complexes) were prepared in buffer containing 25 mM HEPES (pH 7.6), 50 mM NaCl, 1 mM DTT, and 0.5 mM EDTA. The polymerase−DNA complexes were formed by mixing 270 nM DNA substrate with 540 nM wild-type or mutant T4 DNA polymerase. The optimal DNA and enzyme concentrations were determined previously in titration experiments (*15*). With DNA concentrations of 200−600 nM, maximal fluorescence is detected with a 2-fold excess of enzyme if the 3′-end of the template strand is protected from DNA polymerase binding. The sample volume was 60 μL, which was placed in a high-precision, ultra-micro fluorescence cell (Hellma) housed in a temperature-controlled cuvette compartment maintained at 20 ± 0.1 °C. The samples were excited at 315 nm, and emission was collected at 368 nm; a 320 nm long-pass filter was placed between the cuvette and the emission monochromator. A 2 nm band-pass was used for both the excitation and emission monochromators.

Fluorescence Lifetime Measurements. Solutions of 2AP as the free base, in DNA, or in complexes were prepared as for the fluorescence intensity experiments except that the weakly fluorescent DNA solutions were at 2 μM. The temperature in the cuvette compartment was maintained at 20 ± 0.1 °C. The solutions were excited at 315 nm using the frequency-doubled output from a pulsed dye laser (PTI). The PTI LaserStrobe lifetime system is capable of resolving lifetimes as short as 100−200 ps. Fluorescence emission was monitored at 368 nm with a 5 nm band-pass; a 320 nm long-pass filter was inserted between the cuvette and the emission monochromator. The instrument response function was detected at 315 nm using light scattered by a dilute suspension of colloidal silica (Ludox). A stroboscopic optical boxcar method was used for the determination of fluorescence lifetimes (*26*). Decay curves were collected on a time scale of 100 ns, resolved into 1000 channels, and averaged from five repetitive acquisitions. The decay curves were fit to a sum of exponentials

$$I(t) = \sum_{i=1}^{n} \alpha_i e^{-t/\tau_i} \quad (1)$$

using the analysis routine provided by PTI. In eq 1, n is the number of components and τ_i and α_i are the fluorescence lifetime and fractional amplitude values for each of the components, respectively. The quality of curve fits was judged on the basis of the χ^2 value (the acceptable range was 0.9−1.2) and the randomness of residuals, which was assessed statistically by the Durbin−Watson test and by visual inspection.

When the curve fits required more than one exponential term, number-averaged and intensity-averaged lifetimes were calculated using the equations:

$$\langle \tau_{num} \rangle = \sum_{i=1}^{n} \alpha_i \tau_i / \sum_{i=1}^{n} \alpha_i \quad (2)$$

$$\langle \tau_{int} \rangle = \sum_{i=1}^{n} \alpha_i \tau_i^2 / \sum_{i=1}^{n} \alpha_i \tau_i \quad (3)$$

The value τ_{num} is proportional to the quantum yield in the absence of static quenching, and τ_{int} represents the average time that the fluorophore exists in the excited state. Intensity-averaged lifetimes were used for Stern−Volmer analyses (see below) when more than one exponential term was required to fit the decay curves.

Fluorescence Quenching. One microliter of 3 or 6 M acrylamide stock solutions in water was added to 2AP-containing samples equilibrated at 20 °C. After each addition, the steady-state fluorescence intensity and the time-resolved fluorescence decay were recorded. The intensity values were corrected for volume changes.

Fluorescence intensities and lifetimes were fit to the Stern−Volmer equation for collisional quenching:

$$F_0/F = \tau_0/\tau = 1 + K_{SV}[Q] = 1 + k_q \tau_0 [Q] \quad (4)$$

where F_0 and F are the fluorescence intensities in the absence and presence of acrylamide, τ_0 and τ are the intensity-averaged fluorescence lifetimes in the absence and presence of quencher, [Q] is the acrylamide concentration (M), K_{SV} is the Stern−Volmer quenching constant (M^{-1}), and k_q is the bimolecular quenching rate constant (M^{-1} s^{-1}). We report here the effect of acrylamide on 2AP fluorescence in complexes only for dilute solutions of acrylamide up to 0.2 M in order focus on the ability of acrylamide to act as a collisional quencher. Acrylamide may also interfere with formation of enzyme−DNA complexes, which was very apparent for formation of exonuclease complexes with the D219A-DNA polymerase.

RESULTS

Acrylamide Quenching of Fluorescent Exonuclease Complexes Formed with the Wild-Type T4 DNA Polymerase and DNA Substrates Labeled with 2AP at the 3′-End of the Primer Strand. The wild-type T4 DNA polymerase forms highly fluorescent exonuclease complexes with DNA substrates labeled with 2AP at the 3′-end of the primer strand (*20*) and so does the homologous RB69 DNA polymerase (unpublished observations). Since 2AP fluorescence requires

Table 1: Fluorescence Intensities and Lifetimes of the 2AP Base, of 2AP at the 3′-Primer Terminus of ssDNA and dsDNA, and of Binary Complexes Formed with 2AP-Labeled DNAs and the Wild-Type and D219A-DNA Polymerases[a]

2AP base, 2AP-DNA, or complexes	emission intensity (counts/s)	fluorescence lifetimes				
		τ_1 (ns)	τ_2 (ns)	τ_3 (ns)	$\langle\tau_{int}\rangle$ (ns)	$\langle\tau_{num}\rangle$ (ns)
2AP base	67000			11.5 ± 0.2	11.5	11.5
2AP base + 0.2 M acrylamide	4400	0.84 ± 0.02 (0.95)	2.9 ± 0.2 (0.05)		1.1	0.9
2AP-ssDNA	7600	0.4 ± 0.1 (0.38)	3.5 ± 0.1 (0.59)	8.8 ± 0.1 (0.03)	3.8	2.5
2AP-ssDNA + 0.2 M acrylamide	2600	0.8 ± 0.1 (0.76)	1.86 ± 0.05 (0.24)		1.2	1.0
2AP-ssDNA/wtT4	59000			9.89 ± 0.02 (1.0)	9.9	9.9
2AP-ssDNA/wtT4 + 0.2 M acrylamide[b]	56200			9.04 ± 0.02 (1.0)	9.0	9.0
2AP-dsDNA/wtT4	59000			9.74 ± 0.02 (1.0)	9.7	9.7
2AP-dsDNA/wtT4 + 0.2 M acrylamide[b]	51300			8.87 ± 0.02 (1.0)	8.9	8.9
2AP-ssDNA/D219A	20000		3.7 ± 0.3 (0.28)	9.9 ± 0.1 (0.72)	9.1	8.2
2AP-ssDNA/D219A + 0.2 M acrylamide	13000	0.6 ± 0.1 (0.57)	2.9 ± 0.4 (0.20)	9.3 ± 0.1 (0.23)	7.0	3.1
2AP-dsDNA/D219A	11000	0.50 ± 0.05 (0.62)	3.5 ± 0.2 (0.19)	9.8 ± 0.1 (0.19)	7.3	2.8
2AP-dsDNA/D219A + 0.2 M acrylamide	8300	0.55 ± 0.02 (0.77)	3.0 ± 0.2 (0.14)	8.6 ± 0.2 (0.09)	5.2	1.6

[a] Sequences of 2AP-ssDNA and 2AP-dsDNA (2AP at the primer end) are given in Figure 1A. Fluorescence intensities and lifetimes were determined as described in Materials and Methods. The fluorescence intensities reported are for a 2AP concentration of 270 nM for the 2AP base, 2AP in ssDNA or dsDNA, and in complexes formed with 2AP-labeled DNA. The preexponential factors (amplitudes) are indicated in parentheses; errors for amplitudes are ±0.05. [b] The decay curves could also be fit to give two components of about 9 and 0.4 ns, but the amplitude of the 0.4 ns component was <0.15, and there was no significant improvement in the curve fits.

base unstacking, the high fluorescence observed for exonuclease complexes with 2AP at the primer end was attributed to the intercalation of a phenylalanine residue (*14*) as observed in structural studies of exonuclease complexes formed with the RB69 DNA polymerase (*7*). Structural studies also show that a protein shell surrounds the primer end (*4*, *7*), which is expected to shield the primer end from contact with external solvent molecules.

Acrylamide quenching was used to test this proposal for complexes formed in solution. If 2AP at the 3′-end of the primer strand is protected from contact with solvent molecules, then acrylamide will not be able to access 2AP and quench its fluorescence. For controls, we first examined the ability of acrylamide to quench the fluorescence emission of the 2AP free base and ssDNA labeled with 2AP at the 3′-end. (DNAs labeled with 2AP at the 3′-end of the primer strand are described in Figure 1A.) The free 2AP base is highly fluorescent (270 nM yields 67000 counts/s), while 2AP in ssDNA is much less fluorescent (270 nM yields just 8000 counts/s) due to base stacking interactions (Table 1). Acrylamide efficiently quenched the fluorescence emission of both the free base and 2AP in ssDNA (Tables 1 and 2).

Having demonstrated that the free 2AP base and 2AP at the 3′-terminal position of ssDNA can be efficiently quenched by acrylamide, we next tested if 2AP fluorescence is protected from acrylamide quenching when the primer end is bound in the exonuclease active center of the T4 DNA polymerase. The answer is yes. Highly fluorescent exonuclease complexes were formed with the wild-type T4 DNA polymerase and the 2AP-ssDNA substrate (59000 counts/s), and the fluorescence emission was almost completely resistant (>95%) to acrylamide quenching; 0.2 M acrylamide only slightly reduced fluorescence intensity (56200 counts/s) (Table 1). Similar results were observed for exonuclease complexes formed with double-stranded DNA (dsDNA) (Figure 1A) (Table 1).

The small decreases in fluorescence intensity observed for complexes formed with ss- and dsDNA in the presence of acrylamide may indicate that acrylamide interferes with formation of exonuclease complexes with the wild-type T4 DNA polymerase. Since unbound dsDNA is only weakly fluorescent (*11*, *12*, *17*), reducing complex formation will reduce fluorescence intensity. Another possibility is that while the protein pocket surrounding the terminal 2AP in the exonuclease active center largely shields 2AP from contact with acrylamide, some acrylamide molecules may nevertheless penetrate the protein shell and quench 2AP fluorescence. Determining the fluorescence lifetimes of 2AP in complexes in the absence and presence of acrylamide can be used to test these proposals. If acrylamide interferes with complex formation, then the same fluorescence lifetime will be observed with or without acrylamide, but if acrylamide can reach 2AP in the exonuclease active center, then a shorter fluorescence lifetime will be observed.

Table 2: Acrylamide Quenching Parameters[a]

2AP environments	K_{SV} (M^{-1})	k_q($\times 10^9$ M^{-1} s^{-1})
2AP base	67.0	5.7
2AP-ssDNA	10.0	2.6
mmDNA(*n*)/wtT4	2.9	0.5
mmDNA(+1)/wtT4	1.4	0.3
mmDNA(*n*)/D219A	1.2	0.2
AT-DNA(+1)/D219A	3.3	0.4
GC-DNA(+1)/D219A	2.4	0.3

[a] Quenching parameters were determined from acrylamide quench curves as described in Materials and Methods. The DNA substrates are described in Figure 1. The data for complexes formed with the wild-type and D219A-DNA polymerases are presented in Tables 3−5, Figures 2 and 3, and Supporting Information Tables 1−3. 2AP is in the *n* or +1 position in the template strand in mmDNA and in the +1 position in the AT- and GC-DNAs. Exonuclease complexes are expected to be formed with mmDNA. Preexonuclease and preinsertion complexes are formed with the AT-DNA labeled with 2AP at the +1 position. Preinsertion complexes are formed with the GC-DNA.

Fluorescence Lifetimes for 2AP as a Free Base, in 2AP End-Labeled ssDNA, and in 2AP End-Labeled ss- and dsDNAs Bound by the Wild-Type T4 DNA Polymerase. Environment modulates the fluorescence lifetime of 2AP. While a single, relatively long lifetime of 11.5 ns was observed for the free base (Table 1), which is similar to the reported standard of 11.34 ns (*21*), three lifetimes (0.4, 3.5, and 8.8 ns) were detected for 2AP in DNA, which reflect 2AP environments with different degrees of base stacking that are produced by the natural dynamics of ssDNA in

solution (Table 1; *11*, *17*). Similar lifetimes for 2AP in DNA have been reported by others (*11*), but an additional 50 ps lifetime is also observed that cannot be resolved with our instrument. Addition of 0.2 M acrylamide to solutions of the free base or 2AP-labeled ssDNA efficiently quenched fluorescence emission, and the major lifetime components detected were <1 ns (Table 1).

A single fluorescence lifetime was detected for exonuclease complexes formed with the wild-type T4 DNA polymerase and either the ss- or dsDNA substrate labeled with 2AP at the primer end, about 9.7−9.9 ns (Table 1). The relatively long 9.7−9.9 ns fluorescence lifetime observed for 2AP at the terminus of the primer strand bound in the exonuclease active center is near the reported lifetime of the 2AP nucleoside (10.5 ns; *9*, *11*). Thus, 2AP at the primer end of ssDNA bound in the exonuclease active center is in a primarily unstacked conformation as observed for the crystalline state. In a previous study in which exonuclease complexes were formed with a phosphorothioate-modified 2AP-labeled ssDNA substrate, three fluorescence lifetimes were detected instead of the single lifetime observed in our studies, but the major component was characterized by a long fluorescence lifetime of about 10.7 ns (*14*). We suggest that the multiple lifetimes observed for exonuclease complexes in the previous study were caused by the phosphorothioate modification, which may have induced structural perturbations that interfered with DNA binding and/or produced local quenching interactions.

A single lifetime component was again observed for the complexes formed with ss- and dsDNA in the presence of 0.2 M acrylamide, but there was a small decrease in the fluorescence lifetime (Table 1). The addition of 0.2 M acrylamide reduced the fluorescence lifetime for 2AP in complexes formed with ssDNA from 9.9 to 9 ns and from 9.7 to 8.9 ns for complexes formed with dsDNA (Table 1). However, these decreases are small compared to the large decrease in fluorescence lifetime observed for the free base, which decreased from 11.5 ns to the intensity-averaged lifetime value of 1.1 ns (Table 1). Thus, the fluorescence lifetimes provide additional evidence that 2AP at the primer end of DNA bound in the exonuclease active center is protected from acrylamide quenching, but the reduced lifetime in the presence of acrylamide is consistent with the proposal that acrylamide has a weak ability to penetrate the protein shield surrounding the end of the primer strand.

Acrylamide Quenching of Fluorescent Complexes Formed with the Exonuclease-Deficient D219A-DNA Polymerase and DNA Substrates Labeled with 2AP at the 3′-End of the Primer Strand. Under the same conditions as the above experiments with the wild-type T4 DNA polymerase, complexes were formed with the mutant D219A-DNA polymerase. An alanine substitution for aspartate 219 in the exonuclease active center nearly eliminates exonuclease activity (*24*), and the D219A-DNA polymerase has reduced ability to form the highly fluorescent exonuclease complexes detected for the wild-type T4 DNA polymerase with duplex DNA (*20*). Fluorescence emission detected for ssDNA/D219A complexes was just 34% of the intensity detected for ssDNA/wild-type complexes, which indicates that the D219A-DNA polymerase also has difficulty in forming exonuclease complexes with ssDNA (Table 1). A further decrease in emission intensity was observed for complexes formed with dsDNA (Table 1). Fluorescence lifetime measurements were performed to determine the basis for the reduced fluorescence intensity observed for complexes formed with the D219A-DNA polymerase.

Unlike the monoexponential fluorescence decay observed for complexes formed with the wild-type T4 DNA polymerase, the best curve fit to the fluorescence decay detected for ssDNA/D219A complexes required two lifetime components (Supporting Information Figure 1). The longest lifetime component was about 9.9 ns, as observed for exonuclease complexes formed with the wild-type T4 DNA polymerase, but a second component of 3.7 ns was also present (Table 1). In addition, we also predict the presence of totally quenched conformations of 2AP in the complexes formed with the D219A-DNA polymerase, because there was a dramatic decrease in the emission intensity compared to complexes formed with the wild-type T4 DNA polymerase (59000 counts/s for wild-type complexes compared to 20000 counts/s for D219A complexes), but there was only a small decrease in the intensity-averaged lifetimes (9.9 ns for wild-type complexes compared to 9.1 ns for D219A complexes) (Table 1). Such trends usually suggest the presence of dark, nonfluorescent species. Thus, while the D219A-DNA polymerase appears to form fluorescent exonuclease complexes in which the 2AP base is unstacked as observed for the wild-type T4 DNA polymerase, the presence of a fluorescence component characterized by the shorter 3.7 ns lifetime indicates a population of complexes in which 2AP is imperfectly stacked with one or more neighboring bases, and there are additional "dark" complexes in which 2AP is fully base-stacked.

The addition of acrylamide to the 2AP-ssDNA/D219A complexes produced a decrease in the emission intensity of 2AP with increasing acrylamide concentration, but this was due primarily to a decrease in the amplitude of the 9.9 ns lifetime, while the lifetime decreased only marginally (Table 1). Because a decrease in amplitude usually suggests static quenching caused by changes in ground state populations rather than dynamic quenching that occurs in the excited state, we suspect that acrylamide interferes with formation of exonuclease complexes by the mutant DNA polymerase. Since the D219A-DNA polymerase has severely reduced ability to form highly fluorescent exonuclease complexes (Table 1), the addition of acrylamide may further hinder formation of these complexes, which is detected as a decrease in the amplitude of the longest lifetime component. The highly fluorescent exonuclease complexes that are formed, however, are largely resistant to acrylamide quenching as observed for complexes formed with the wild-type T4 DNA polymerase.

The D219A-DNA polymerase was able to form even fewer highly fluorescent exonuclease complexes with the dsDNA substrate compared to ssDNA (Table 1). The amplitude of the longest lifetime component decreased from 0.72 to 0.19 for complexes formed with dsDNA compared to ssDNA (Table 1). An intermediate lifetime component (3.5 ns) was detected as observed for complexes formed with the ssDNA, but the predominant component had a lifetime of just 0.5 ns. The addition of 0.2 M acrylamide produced a modest quench in fluorescence emission that was due primarily to a decrease in the lifetime and amplitude of the longest lifetime component. We conclude from these experiments that

Table 3: Positional Dependence of Fluorescence for 2AP in the Template Strand in Complexes Formed with the Wild-Type T4 DNA Polymerase and Mismatched (mm) DNA Substrates[a]

2AP position[a]	fluorescence emission intensity[b] (counts/s)	fluorescence enhancement (*x*-fold)
WT/*n*	13000	4.6
WT/+1	10300	5.0
WT/+2	6080	3.6
WT/+3	4400	2.4
unbound mmDNA	1700−2800[c]	

[a] The mmDNA substrates are described in Figure 1A. [b] The emission intensities are for complexes formed with 270 nM DNA and 540 nM wild-type T4 DNA polymerase as described in Materials and Methods. [c] The emission intensities are for unbound mmDNAs for 2AP in the *n* (2800 counts/s), +1 (2040 counts/s), +2 (1700 counts/s), and +3 (1850 counts/s) positions.

although the D219A-DNA polymerase can apparently form highly fluorescent exonuclease complexes characterized by the 9.7−9.9 ns lifetime as observed for the wild-type T4 DNA polymerase, the mutant DNA polymerase has severely reduced ability to do so, particularly with the dsDNA substrate.

Fluorescent Exonuclease Complexes Formed with the Wild-Type T4 DNA Polymerase and DNA Substrates Labeled with 2AP in the Template Strand. 2AP was placed in either the base-pairing *n* position in the template strand or at the more distal +1, +2, or +3 positions (Figure 1A). In order to force formation of exonuclease complexes, the primer end was terminated with two mismatches to form mismatched DNA (mmDNA) (*17*). 2AP fluorescence intensity was enhanced when the wild-type T4 DNA polymerase formed exonuclease complexes with the mmDNA substrates: the enhancement was about 5-fold for 2AP in the *n* and +1 positions, which decreased to <4-fold for 2AP at the +2 position and was only 2.4-fold for 2AP at the +3 position (Table 3).

The time-resolved fluorescence decay curve observed for exonuclease complexes formed with the mmDNA substrate labeled at the *n* position required three lifetime components to obtain a good fit of 0.8, 3.4, and 9.0 ns (Table 4). Fluorescence enhancement above unbound mmDNA was due to increases in the amplitudes of the longest and intermediate lifetime components. Because it is likely that predominantly exonuclease complexes are formed with the mmDNA and the wild-type T4 DNA polymerase, the presence of three lifetime components suggests that 2AP can be in different local environments in exonuclease complexes with varying degrees of base stacking interactions from relatively unstacked (9.0 ns component), imperfectly stacked (3.4 ns component), nearly fully stacked (0.8 ns component), and fully stacked (dark, undetectable components). A similar lifetime profile was observed for 2AP in the +1 position (Supporting Information Table 1). The different 2AP environments could be rapidly interconverting because Larsen et al. (*27*) propose that 2AP in ssDNA can convert from a well-quenched dark state to a state with a lifetime in the nanosecond range in just 30−40 ps. The enzyme can increase localized base unstacking by bending and/or stretching the DNA. The region of fluorescence enhancement appears to be restricted to residues from the *n* to +3 positions (Table 3) and also the −1 position may be included, as suggested by a previous experiment (*14*).

Accessibility of 2AP in the *n* and +1 positions in the template strand to acrylamide in exonuclease complexes was determined (Table 4, Supporting Information Table 1). The Stern−Volmer plot for acrylamide quenching of 2AP fluorescence in exonuclease complexes was approximately linear (Figure 2), and the Stern−Volmer constant calculated for 2AP in the *n* position of the template strand was $K_{SV} = 2.9\ M^{-1}$ (Table 2). The ratio of lifetimes (τ_0/τ) also increased approximately linearly and proportionately with the F_0/F ratio with increasing acrylamide concentration (Figure 2), which indicates that quenching was primarily by a diffusive/collisional quenching process. Note, however, that we cannot rule out the possibility of a minor static quenching component because acrylamide may interfere with complex formation especially for the D219A-DNA polymerase; this point applies to all of the studies with acrylamide (Figures 2 and 3). The quenching rate constant k_q calculated from the Stern−Volmer plot was $0.5 \times 10^9\ M^{-1}\ s^{-1}$ (Table 2). Smaller quenching parameters were observed for exonuclease complexes formed with mmDNA labeled at the +1 position with 2AP (Table 2), which indicates that 2AP in the +1 position is more shielded from contact with acrylamide than for 2AP in the *n* position. Both K_{SV} and k_q were reduced in complexes formed with the mmDNA substrates compared to the unbound ssDNA with 2AP at the primer end (Table 2), which indicates that while 2AP in the template strand in exonuclease complexes is exposed to the external solvent, the DNA polymerase partially shields 2AP from contact with acrylamide molecules.

Fluorescent Exonuclease Complexes Formed with the Exonuclease-Deficient D219A-DNA Polymerase and DNA Substrates Labeled with 2AP in the Template Strand. The steady-state fluorescence emission intensities and fluorescence decays of 2AP-mmDNA(*n*)/wtT4 and 2AP-mmDNA(*n*)/D219A complexes in the absence of acrylamide were similar (Tables 4 and 5), but the complexes formed with the mutant DNA polymerase were more resistant to acrylamide quenching as shown by the Stern−Volmer plots of F_0/F and τ_0/τ (Figure 2). The quenching parameters for complexes formed with the D219A-DNA polymerase were significantly lower: $K_{SV} = 1.2\ M^{-1}$ and $k_q = 0.2 \times 10^9\ M^{-1}\ s^{-1}$ (Table 2). Thus, 2AP in the *n* position in complexes formed with mmDNA was more accessible to acrylamide in complexes formed with the wild-type T4 DNA polymerase than with the D219A-DNA polymerase, which indicates that the complexes are not structurally identical.

Acrylamide Quenching of Preexonuclease Complexes. T4 DNA polymerase forms several different complexes during the course of the nucleotide incorporation pathway: complexes poised to bind the next incoming nucleotide, complexes involved in checking the accuracy of the incoming nucleotide, complexes performing the chemistry reaction, and complexes that have just incorporated a nucleotide but have not yet translocated to be in position to bind the next nucleotide (*1*, *2*, *15*). In previous studies we observed that the T4 DNA polymerase formed highly fluorescent complexes with DNA substrates labeled at the +1 template position (Figure 1B) as well as less fluorescent complexes (*15*). Higher fluorescence intensities were observed for complexes formed with A+T-rich compared to G+C-rich DNAs (*15*) due to the presence of a 10.5 ns lifetime component that was detected for complexes formed with

Table 4: Acrylamide Quenching of Exonuclease Complexes Formed with the Wild-Type T4 DNA Polymerase and mmDNA Labeled with 2AP at the *n* Position in the Template Strand[a]

acrylamide concn (M)	emission intensity (counts/s)	fluorescence lifetimes τ_1 (ns)	τ_2 (ns)	τ_3 (ns)	$\langle\tau_{int}\rangle$ (ns)
0	13000	0.8 ± 0.1 (0.50)	3.4 ± 0.1 (0.36)	9.0 ± 0.1 (0.14)	5.5
0.025	12250	1.0 ± 0.1 (0.58)	3.6 ± 0.4 (0.27)	8.4 ± 0.3 (0.15)	5.2
0.050	11460	0.9 ± 0.1 (0.60)	3.3 ± 0.1 (0.26)	8.0 ± 0.1 (0.14)	4.9
0.075	10970	0.8 ± 0.1 (0.59)	3.2 ± 0.1 (0.27)	7.6 ± 0.2 (0.14)	4.7
0.100	10540	0.7 ± 0.1 (0.65)	3.0 ± 0.3 (0.22)	7.4 ± 0.2 (0.13)	4.5
0.150	9600	0.7 ± 0.1 (0.62)	2.4 ± 0.3 (0.24)	6.8 ± 0.1 (0.14)	4.2
0.200	8900	0.5 ± 0.1 (0.69)	1.8 ± 0.2 (0.19)	6.4 ± 0.1 (0.12)	3.9

[a] The sequence of the mmDNA with 2AP in the *n* position is shown in Figure 1. The amplitudes are indicated in parentheses. The lifetimes and amplitudes for unbound mmDNA are the following: $\tau_1 = 0.8$ (0.79); $\tau_2 = 3.3$ (0.19); $\tau_3 = 8.5$ (0.02).

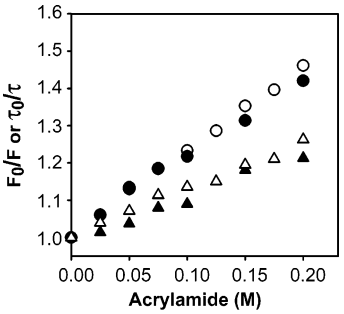

FIGURE 2: Stern−Volmer plots for acrylamide quenching of mmDNA/wtT4 complexes (○, ●) and mmDNA/D219A complexes (△, ▲). 2AP is in the *n* position in the template strand. Open symbols indicate F_0/F ratios; closed symbols indicate τ_0/τ ratios. The curves are plotted from data presented in Table 4 (wild-type T4 DNA polymerase) and Table 5 (D219A-DNA polymerase).

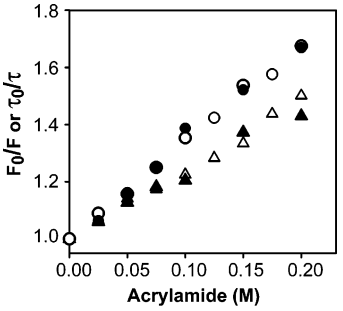

FIGURE 3: Stern−Volmer plots for acrylamide quenching of AT-DNA/D219A complexes (○, ●) and GC-DNA/D219A complexes (△, ▲). Open symbols indicate F_0/F ratios; closed symbols indicate τ_0/τ ratios. The curves are plotted from data presented in Supporting Information Table 2 (A+T-rich DNA) and Supporting Information Table 3 (G+C-rich DNA).

A+T-rich but not the G+C-rich DNA substrates (*17*). We proposed that complexes characterized by the 10.5 ns component were preexonuclease complexes because formation of these complexes increased under conditions predicted to trap preexonuclease complexes: DNA substrates with an A+T-rich primer terminal region, which favors proofreading; absence of dNTPs; and mutant DNA polymerases with reduced ability to form exonuclease complexes. A second long lifetime component of about 8.3 ns was also detected for complexes formed with A+T-rich DNA substrates (*17*). When complexes were formed with G+C-rich DNA substrates, which favor primer elongation rather than proofreading, 8.3 ns was the longest lifetime component detected. We proposed that the fluorescent complexes characterized by the 8.3 ns lifetime were nucleotide preinsertion complexes because this component was detected for the G+C-rich DNA, which favors nucleotide incorporation over proofreading, and because the addition of low amounts of dTTP/Mg^{2+} to complexes formed with the A+T-rich DNA increased the amplitude of the 8.3 ns component at the expense of the 10.5 ns component (*17*).

These experiments were repeated with the exonuclease-deficient D219A-DNA polymerase (Supporting Information Tables 2 and 3). As observed previously with another exonuclease-deficient DNA polymerase, fluorescence intensity of complexes formed with the A+T-rich DNA (Figure 1B) was higher than detected for complexes formed with the G+C-rich DNA, which was due to the large contribution from the 10.9 ns lifetime component that was absent in the decay of complexes formed with the G+C-rich DNA. The longest lifetime detected for GC-DNA/D219A complexes was 9.4 ns, which could be an average lifetime of two long lifetime components: an 8.5 ns component with a small contribution from the longer 10.9 ns component that cannot be resolved.

We extended our previous findings by determining if 2AP fluorescence in these complexes was sensitive to acrylamide quenching. The acrylamide titration plots of the ratio of fluorescence intensities (F_0/F) increased approximately linearly for both the AT-DNA/D219A and GC-DNA/D219A complexes, and the ratio of lifetimes (τ_0/τ) increased proportionately as expected for a diffusive (collisional) quenching process (Figure 3). Quenching parameters were calculated from the plots: $K_{SV} = 3.3\ M^{-1}$ and $k_q = 0.4 \times 10^9\ M^{-1}\ s^{-1}$ for AT-DNA/D219A complexes and $K_{SV} = 2.4\ M^{-1}$ and $k_q = 0.3 \times 10^9\ M^{-1}\ s^{-1}$ for GC-DNA/D219A complexes (Table 2). For both the AT-DNA/D219A and GC-DNA/D219A complexes, acrylamide quenching was associated with quenching of the longest lifetime components of 8.5−10.5 ns (Supporting Information Tables 2 and 3). For AT-DNA/D219A complexes, both the 10.9 and 8.5 ns components were sensitive to acrylamide, but note that these components could not be resolved in the presence of acrylamide due to the presence of quenched products (Supporting Information Table 2). The two other fluorescent components detected for the AT and GC complexes were characterized by fluorescence lifetimes of about 3 and 0.7−0.8 ns, but these components were not sensitive to acrylamide (Supporting Information Tables 2 and 3). The similar quenching rate constants of about $0.3-0.4 \times 10^9\ M^{-1}\ s^{-1}$ (Table 2) for complexes formed with the AT- and GC-DNA

Table 5: Acrylamide Quenching of Complexes Formed with the Exonuclease-Deficient D219A-DNA Polymerase and mmDNA Labeled with 2AP at the *n* Position in the Template Strand[a]

		fluorescence lifetimes			
acrylamide concn (M)	emission intensity (counts/s)	τ_1 (ns)	τ_2 (ns)	τ_3 (ns)	$\langle\tau_{int}\rangle$ (ns)
0	13000	0.9 ± 0.1 (0.50)	3.5 ± 0.2 (0.36)	9.2 ± 0.2 (0.14)	5.5
0.025	12670	0.8 ± 0.1 (0.56)	3.7 ± 0.2 (0.30)	8.7 ± 0.3 (0.15)	5.4
0.050	12340	0.9 ± 0.1 (0.54)	3.4 ± 0.3 (0.32)	8.7 ± 0.3 (0.14)	5.3
0.075	12100	0.9 ± 0.1 (0.54)	3.4 ± 0.2 (0.34)	8.8 ± 0.3 (0.12)	5.1
0.100	11780	0.7 ± 0.1 (0.51)	3.1 ± 0.1 (0.36)	8.5 ± 0.2 (0.13)	5.0
0.150	11340	0.8 ± 0.1 (0.55)	3.2 ± 0.2 (0.34)	8.2 ± 0.3 (0.11)	4.7
0.200	11100	0.7 ± 0.1 (0.57)	3.3 ± 0.3 (0.33)	8.1 ± 0.4 (0.10)	4.5

[a] The sequence of the mmDNA with 2AP in the *n* position is shown in Figure 1. The amplitudes are indicated in parentheses. The lifetimes and amplitudes for unbound mmDNA are the following: $\tau_1 = 0.8$ (0.79); $\tau_2 = 3.3$ (0.19); $\tau_3 = 8.5$ (0.02).

substrates indicate that both long lifetime components were equally accessible to acrylamide.

DISCUSSION

The mechanism of active site switching during proofreading is not completely understood, but the overall process must minimize extension of a mismatched primer terminus, separate the end of the primer strand from the template, remove the terminal nucleotide, and then return the trimmed end to the polymerase active center without misaligning the primer and template strands. Our genetic and biochemical studies indicate that amino acid residues in four of the five protein domains of the T4 DNA polymerase are required (*3*, *5*, *25*, *28*). Structural studies of the RB69 DNA polymerase (*4*) reveal that polymerase-to-exonuclease active site switching requires loss of extensive protein interactions in the polymerase active center between residues in the palm domain with the phosphodiester backbone of the four terminal base pairs of the primer strand, which are replaced by new interactions with residues in the exonuclease domain (*4*). Protein interactions with the template strand in exonuclease complexes cannot be determined, however, because the five terminal nucleotides at the 5′-end of the template strand are disordered (*4*). The template strand may be disordered because there is strand movement and/or the five nucleotides of the single-stranded template overhang may not be long enough for the polymerase to form stable contacts with the template strand. The DNA substrates used in our studies, which have from 12 to 15 nucleotides of overhanging template DNA (Figure 1), allow T4 DNA polymerase interactions with the template strand to be assessed. We have also compared complex formation in solution with the wild-type T4 DNA polymerase to the exonuclease-deficient D219A-DNA polymerase.

Although the experiments reported here were performed in the absence of Mg^{2+} in order to protect the DNA substrates from degradation by the potent T4 DNA polymerase exonuclease activity, formation of the fluorescent complexes is independent of Mg^{2+}. In reactions with 2AP initially in the +2 position in the template strand, a large increase in fluorescence intensity is observed when the primer end is extended by one nucleotide to place 2AP in the +1 position to form the highly fluorescence +1 complexes (*16*). Further primer elongation in which a dTMP is incorporated opposite template 2AP leads to a decrease in fluorescence intensity, which is due to nucleotide incorporation and subsequent formation of less fluorescent exonuclease complexes (*16*). In addition, the previously reported need for Mg^{2+} for partitioning between the polymerase and exonuclease active sites of the T4 DNA polymerase (*14*) must be reevaluated because a hydrolysis-resistant phosphorothioate DNA was used. Structural studies of the Klenow fragment indicate that hydrolysis resistance is due to steric hindrance by the bulky sulfur atom: the S_p phosphorothioate isomer cannot be bound in the exonuclease active site in conjunction with metal ions (*29*). If this mechanism for hydrolysis resistance extends to the T4 DNA polymerase, which is likely, then the addition of Mg^{2+} will reduce formation of exonuclease complexes with the phosphorothioate DNA. Furthermore, any exonuclease complexes formed will be in the absence of bound Mg^{2+} in the exonuclease active site even though Mg^{2+} is present in solution. Thus, Mg^{2+} is not essential for active site partitioning; increased partitioning to the polymerase active center was observed with the phosphorothioate DNA because Mg^{2+} interfered with formation of exonuclease complexes. For these reasons we believe that the solvent exposure values reported here for 2AP, which were determined in the absence of Mg^{2+}, are applicable to complexes formed in the presence of Mg^{2+}.

Fluorescence studies of exonuclease complexes formed with the wild-type T4 DNA polymerase labeled with 2AP in the 3′-terminal position of the primer strand are fully consistent with structural studies. A single lifetime of about 9.7−9.9 ns was observed (Table 1), which indicates (1) that a homogeneous conformational state of 2AP can be attained in exonuclease complexes under solution conditions and (2) that 2AP positioned at the primer end in exonuclease complexes is free of base stacking interactions, as expected if a phenylalanine residue intercalates between the two terminal bases (*4*, *7*). Structural studies also show that the primer terminus is buried in a protein pocket, which is expected to protect the terminal base from interactions with acrylamide; this was observed (Table 1).

The exonuclease-deficient D219A-DNA polymerase, however, behaved differently. Although the D219A-DNA polymerase formed highly fluorescent exonucleases complexes characterized by the 9.9 ns lifetime component with the 2AP 3′-end-labeled ssDNA, a component with an intermediate lifetime (3.5−3.7 ns) was also detected (Table 1). The 3.5−3.7 ns component was also observed for complexes formed with dsDNA, but only a small amount of the 9.9 ns component was detected; the predominant component was characterized by a very short lifetime, just 0.5 ns (Table 1). These observations together indicate that the D219A-DNA

polymerase has severely reduced ability to form the highly fluorescent exonuclease complexes characterized by the 9.7−9.9 ns lifetime, particularly with dsDNA. Thus, the D219A substitution affects not only Mg^{2+} binding in the exonuclease active center but also the ability to form stable exonuclease complexes in which the terminal base is unstacked.

Acrylamide appeared to further hinder the ability of the D219A-DNA polymerase to form the highly fluorescent exonuclease complexes. While collisional quenching is expected to reduce both the lifetime and the amplitude of the fluorophore, acrylamide reduced primarily the amplitude of the 9.8−9.9 ns component formed with the D219A-DNA polymerase (Table 1), which suggests that acrylamide interfered with the ability of the mutant enzyme to form fluorescent complexes.

Interestingly, not all alanine substitutions for conserved aspartate residues in the exonuclease active center equally decrease the ability of the T4 DNA polymerase to form highly fluorescent exonuclease complexes with 2AP end-labeled DNA. There are three conserved aspartate residues in the exonuclease active site that are required for catalytic activity: D112, D219, and D324; alanine substitutions for each individual aspartate residue eliminates or nearly eliminates exonuclease activity (*24*). While the D219A substitution severely reduces formation of fluorescent exonuclease complexes (Table 1; *20*), only a 1.5-fold reduction is detected for the D112A/E114A-DNA polymerase (*20*) and no reduction is observed for the D324A-DNA polymerase (unpublished observations). We observed that mutant DNA polymerases with reduced ability to form exonuclease complexes form preexonuclease complexes instead (*17*). Thus, the D219A-DNA polymerase was used here for studies of preexonuclease complexes (Figure 3) while the wild-type T4 DNA polymerase was used for studies of exonuclease complexes in which the 2AP-labeled primer end is bound in the exonuclease active center (Table 1).

What happens to the template strand when the primer end is bound in the exonuclease active center? For exonuclease complexes formed with the wild-type T4 DNA polymerase and mmDNA substrates, a 4−5-fold fluorescence enhancement above unbound DNA was observed for 2AP in the *n*, +1, and +2 positions, and smaller enhancements were detected for the +3 and −1 positions (Table 3; *14*). The fluorescence enhancement was due to increases in the amplitudes of the longest and intermediate lifetime components, 9 and 3.4 ns (Table 4), compared to the unbound mmDNA. These observations suggest that the DNA polymerase holds the template strand in a way to produce position-dependent base unstacking in the template strand in exonuclease complexes. If the template strand were not held, then fluorescence enhancement above unbound ssDNA would not be seen. 2AP fluorescence in the *n* and +1 positions in the template strand was quenched by acrylamide (Figure 2, Table 4, Supporting Information Table 1), but quenching was less efficient for complexes compared to unbound DNA (Table 2), which indicates that the protein is restricting access. This restricted access is consistent with structural studies of a ternary complex of the RB69 DNA polymerase, DNA, and nucleotide in which the DNA is shown to sit in a protein cleft and is thus largely protected from the external solvent except on one side (*30*).

The D219A-DNA polymerase appeared to form similar fluorescent complexes with the mmDNA with 2AP in the *n* position as observed for the wild-type T4 DNA polymerase. The fluorescence intensities and fluorescence lifetimes detected for the complexes formed with the two DNA polymerases were essentially identical (Tables 4 and 5). Although the D219A-DNA polymerase had severely reduced ability to form the highly fluorescent exonuclease complexes with the dsDNA substrate labeled on the primer end with 2AP (Table 1), the presence of two preformed terminal mismatches in the mmDNA substrate appeared to assist the D219A-DNA polymerase in forming exonuclease complexes. However, despite the similar fluorescent properties of the complexes formed with mmDNA and the wild-type and mutant DNA polymerases (Tables 4 and 5), the complexes formed with the D219A-DNA polymerase were more resistant to acrylamide quenching (Figure 2, Table 5), which indicates that the complexes are not identical.

What happens to the template strand *before* the primer end is transferred to the exonuclease active center? We confirm here what we reported previously (*15*−*17*): the DNA polymerase unstacks the base in the +1 position. Base unstacking could be produced if the template strand is bent as observed in the ternary structure of the RB69 DNA polymerase (*30*), or the base/nucleoside may be flipped to an extrahelical position as observed for some family A DNA polymerases (*31*). Irrespective of mechanism, a unique fluorescent component with a 10.9 ns lifetime is detected in complexes formed with the D219A-DNA polymerase and the A+T-rich DNA substrate that is not detected for complexes formed with the G+C-rich DNA (Figure 1B, Supporting Information Tables 2 and 3). The reduced ability of the D219A-DNA polymerase to form exonuclease complexes, the A+T-richness of the DNA substrate, and the absence of dNTPs allow a relatively large population of preexonuclease complexes to be formed. Preexonuclease complexes are in equilibrium with other types of complexes including preinsertion complexes that are characterized by a 8.5 ns lifetime (*17*). Both long lifetime components were subject to acrylamide quenching (Figure 3, Supporting Information Tables 2 and 3), which suggests that 2AP in both preexonuclease and preinsertion complexes may be equally exposed to solvent. Structurally, the preexonuclease complexes may resemble the hybrid polymerase/exonuclease structure reported for the exonuclease-deficient D222A/D327A-RB69 DNA polymerase with a tetrahydrofuran in the *n* position of the template strand (*4*, *32*). In these complexes the template/primer is bound in the polymerase active center, the DNA polymerase has not translocated, the short template strand overhang is bent, and minor groove interactions are lost.

Summary: Polymerase-to-Exonuclease Switching Pathway. We have detected formation of a highly fluorescent complex for 2AP in the +1 position in the template strand that takes place just before the chemistry step of nucleotide incorporation (*2*, *16*, *17*). Unstacking of the base in the +1 position will help to prevent the misuse of this and more distal bases as possible templates as suggested for a mechanism to prevent frame-shift mutations (*33*). After the nucleotide is incorporated, the DNA polymerase may translocate to be in position to bind the next incoming nucleotide, but if a wrong nucleotide is incorporated, we propose that

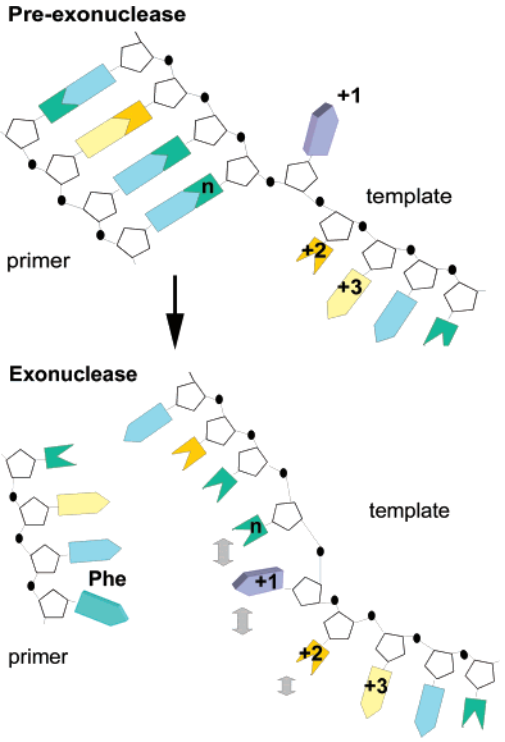

FIGURE 4: Polymerase-to-exonuclease switching: template strand dynamics. Full base unstacking is detected for 2AP in the +1 position of the template strand in preexonuclease complexes (*17*). The mechanism for base unstacking is unknown, but strand bending and base flipping have been detected in structural studies of DNA polymerase complexes (*30*, *31*). Partial base unstacking is observed in the template strand of exonuclease complexes, primarily for 2AP at the *n* and +1 positions (as indicated by the double-headed arrows). By holding the template strand while the primer strand is transferred back and forth between the polymerase and exonuclease active centers, the DNA polymerase can maintain the correct alignment of the primer and template strands to prevent frameshift mutations and to allow efficient resumption of DNA replication. A phenylalanine residue (Phe) is shown to intercalate between the two terminal bases of the primer strand in exonuclease complexes. Other protein interactions are not illustrated.

the base in the +1 position remains unstacked and a preexonuclease complex is formed (Figure 4). The precise structure of the unstacked base is not known, but the long 10.9 ns lifetime (Supporting Information Table 2) indicates that 2AP in the +1 position in these complexes is fully free of contacts with the adjacent bases, but only a little base unstacking is observed for the base at the +2 position (*15*); thus, only the base in the +1 position is illustrated as unstacked.

Base unstacking at the +1 position is expected to deter translocation, which allows an opportunity for the primer end to be separated from the template strand and transferred to the exonuclease active center by a process that requires a β-hairpin structure in the exonuclease domain (*3*, *5*, *25*, *28*). Structural studies indicate that the hairpin interacts with apparent preexonuclease complexes in which the primer/template is bound in the polymerase active center and may move with the primer end as the primer strand is separated from the template and transferred to the exonuclease active center (*4*). Amino acid substitutions in the hairpin of the T4 DNA polymerase (*25*, *28*) or shortening the hairpin of the RB69 DNA polymerase (*34*) reduces the ability of the mutant DNA polymerases to form exonuclease complexes.

The fluorescence studies demonstrate that while 2AP in the +1 position of the template strand is fully unstacked at the beginning of the proofreading pathway in preexonuclease complexes, 2AP base stacking interactions are partially restored when the primer end is bound in the exonuclease active center. Compared to preexonuclease complexes where 2AP at the +1 position is fully unstacked to produce a fluorescence lifetime of 10.9 ns, smaller 4−5-fold enhancements were detected for 2AP in the *n* and +1 positions (Table 3). Double-headed arrows are used in Figure 4 to illustrate base unstacking for the bases at the *n* and +1 positions and, to a smaller extent, for the base at the +2 position. Because base unstacking in the template strand of exonuclease complexes is position dependent, the DNA polymerase appears to hold the template strand. This holding will allow the DNA polymerase to maintain the correct alignment of the primer and template strands so that when the trimmed primer end is returned to the polymerase active center, the enzyme will be in correct position to resume nucleotide incorporation.

ACKNOWLEDGMENT

We thank Chithra Hariharan, Matthew Hogg, and Usharani Subuddhi for helpful comments on the manuscript.

SUPPORTING INFORMATION AVAILABLE

Figure 1 presenting the residual analyses for single and double exponential fits of the decay curves for complexes formed with the wild-type and D219A-DNA polymerases with ssDNA labeled at the primer end with 2AP, Table 1 providing the data for acrylamide quenching of exonuclease complexes formed with the wild-type T4 DNA polymerase and mmDNA labeled with 2AP at the +1 position, and Tables 2 and 3 providing the data for Figure 3. This material is available free of charge via the Internet at http://pubs.acs.org.

REFERENCES

1. Capson, T. L., Peliska, J. A., Kaboord, B. F., Frey, M. W., Lively, C., Dahlberg, M., and Benkovic, S. J. (1992) Kinetic characterization of the polymerase and exonuclease activities of the gene 43 protein of bacteriophage T4, *Biochemistry 31*, 10984−10994.
2. Hariharan, C., Bloom, L. B., Helquist, S. A., Kool, E. T., and Reha-Krantz, L. J. (2006) Dynamics of nucleotide incorporation: snapshots revealed by 2-aminopurine fluorescence studies, *Biochemistry 45*, 2836−2844.
3. Stocki, S. A., Nonay, R. L., and Reha-Krantz, L. J. (1995) Dynamics of bacteriophage T4 DNA polymerase function: Identification of amino acid residues that affect switching between polymerase and 3′→5′ exonuclease activities, *J. Mol. Biol. 254*, 15−28.
4. Hogg, M., Wallace, S. S., and Doublié, S. (2004) Crystallographic snapshots of a replication DNA polymerase encountering an abasic site, *EMBO J. 23*, 1483−1493.
5. Reha-Krantz, L. J., Marquez, L. A., Elisseeva, E., Baker, R. P., Bloom, L. B., Dunford, H. B., and Goodman, M. F. (1998) The proofreading pathway of bacteriophage T4 DNA polymerase, *J. Biol. Chem. 273*, 22969−22976.
6. Reddy, M. K., Weitzel, S. E., and von Hippel, P. H. (1992) Processive proofreading is intrinsic to the T4 DNA polymerase, *J. Biol. Chem. 267*, 14157−14166.
7. Shamoo, Y., and Steitz, T. A. (1999) Building a replisome from interacting pieces: Sliding clamp complexed to a peptide from DNA polymerase and a polymerase editing complex, *Cell 99*, 155−166.
8. Hogg, M., Cooper, W., Reha-Krantz, L., and Wallace, S. S. (2006) *Nucleic Acids Res. 34*, 2538−2535.

9. Rachofsky, E. L., Osman, R., and Ross, J. B. (2001) Probing structure and dynamics of DNA with 2-aminopurine: Effects of local environment on fluorescence, *Biochemistry 40*, 946−956.
10. Neely, R. K., Daujotyte, D., Grazulis, S., Magennis, S. W., Dryden, D. T. F., Klimašauskas, and Jones, A. C. (2005) Time-resolved fluorescence of 2-aminopurine as a probe of base flipping in M.HhaI-DNA complexes, *Nucleic Acids Res. 33*, 6953−6960.
11. Guest, C. R., Hochstrasser, R. A., Sowers, L C., and Millar, D. P. (1991) Dynamics of mismatched base pairs in DNA, *Biochemistry 30*, 3271−3279.
12. Jean, J. M., and Hall, K. B. (2001) 2-Aminopurine fluorescence quenching and lifetimes: Role of base stacking, *Proc. Natl. Acad. Sci. U.S.A. 98*, 37−41.
13. Nordlund, T. M., Andersson, S., Nilsson, L., Rigler, R., Gräslund, A., and McLaughlin, L. W. (1989) Structure and dynamics of a fluorescent DNA oligomer containing the EcoRI recognition sequence: fluorescence, molecular dynamics, and NMR studies, *Biochemistry 28*, 9095−9103.
14. Beechem, J. M., Otto, M. R., Bloom, L. B., Eritja, R., Reha-Krantz, L. J., and Goodman, M. F. (1998) Exonuclease-polymerase active site partitioning of primer-template DNA strands and equilibrium Mg^{2+} binding properties of bacteriophage T4 DNA polymerase, *Biochemistry 37*, 10144−10155.
15. Mandal, S. S., Fidalgo da Silva, E., and Reha-Krantz, L. J. (2002) Using 2-aminopurine fluorescence to detect base unstacking in the template strand during nucleotide incorporation by the bacteriophage T4 DNA polymerase, *Biochemistry 41*, 4399−4406.
16. Fidalgo da Silva, E., Mandal, S. S., and Reha-Krantz, L. J. (2002) Using 2-aminopurine fluorescence to measure incorporation of incorrect nucleotides by wild type and mutant bacteriophage T4 DNA polymerases, *J. Biol. Chem. 277*, 40640−40649.
17. Hariharan, C., and Reha-Krantz, L. J. (2005) Using 2-aminopurine fluorescence to detect bacteriophage T4 DNA polymerase-DNA complexes that are important for primer extension and proofreading reactions, *Biochemistry 44*, 15674−15684.
18. Clayton, L. K., Goodman, M. F., Branscomb, E. W., and Galas, D. J. (1979) Error induction and correction by mutant and wild type T4 DNA polymerases. Kinetic error discrimination mechanisms, *J. Biol. Chem. 254*, 1902−1979.
19. Bessman, M. J., and Reha-Krantz, L. J. (1977) Studies on the biochemical basis of spontaneous mutation. V. Effect of temperature on mutation frequency, *J. Mol. Biol. 116*, 115−123.
20. Bloom, L. B., Otto, M. R., Eritja, R., Reha-Krantz, L. J., Goodman, M. F., and Beechem, J. M. (1994) Pre-steady-state kinetic analysis of sequence-dependent nucleotide excision by the 3′-exonuclease activity of bacteriophage T4 DNA polymerase, *Biochemistry 33*, 7576−7586.
21. Lakowicz, J. R. (1999) *Principles of Fluorescence Spectroscopy*, 2nd ed., p 10013, Plenum Publishers, New York.
22. Braithwaite, D. K., and Ito, J. (1993) Compilation, alignment, and phylogenetic relationships of DNA polymerases, *Nucleic Acids Res. 21*, 787−802.
23. Reha-Krantz, L. J., Nonay, R. L., and Stocki, S. (1993) Bacteriophage T4 DNA polymerase mutations that confer sensitivity to the PPi analog phosphonoacetic acid, *J. Virol. 67*, 60−66.
24. Elisseeva, E., Mandal, S. S., and Reha-Krantz, L. J. (1999) Mutational and pH studies of the 3′→5′ exonuclease activity of bacteriophage T4 DNA polymerase, *J. Biol. Chem. 274*, 25151−25158.
25. Marquez, L. A., and Reha-Krantz, L. J. (1996) Using 2-aminopurine fluorescence and mutational analysis to demonstrate an active role of bacteriophage T4 DNA polymerase in strand separation required for 3′→5′ exonuclease activity, *J. Biol. Chem. 271*, 28903−28911.
26. James, D. R., Siemiarczuk, A., and Ware, W. T. (1992) Stroboscopic optical boxcar technique for the determination of fluorescence lifetimes, *Rev. Sci. Instrum. 63*, 1710−1716.
27. Larsen, O. F. A., van Stokkum, I. H. M., de Weerd, F. L., Vengris, M., Aravindakumar, C. T., van Grondelle, R., Geacintov, N. E., and van Amerongen, H. (2004) Ultrafast transient-absorption and steady-state fluorescence measurements on 2-aminopurine substituted dinucleotides and 2-aminopurine substituted DNA duplexes, *Phys. Chem. Chem. Phys. 6*, 154−160.
28. Baker, R. P., and Reha-Krantz, L. J. (1998) Identification of a transient excision intermediate at the crossroads between DNA polymerase extension and proofreading pathways, *Proc. Natl. Acad. Sci. U.S.A. 95*, 3507−3512.
29. Brautigam, C. S., and Steitz, T. A. (1998) Structural principles for the inhibition of the 3′-5′ exonuclease activity of *Escherichia coli* DNA polymerase I by phosphorothioates, *J. Mol. Biol. 277*, 363−377.
30. Franklin, M. C., Wang, J., and Steitz, T. A. (2001) Structure of the replicating complex of a pol α family DNA polymerase, *Cell 105*, 657−667.
31. Li, Y., Korolev, S., and Waksman, G. (1998) Crystal structures of open and closed forms of binary and ternry complexes of the large fragment of *Thermus aquaticus* DNA polymerase I: structural basis for nucleotide incorporation, *EMBO J. 17*, 7514−7525.
32. Freisinger, E., Grollman, A. P., Miller, H., and Kisker, C. (2004) Lesion (in)tolerance reveals insights into DNA replication fidelity, *EMBO J. 23*, 1494−1505.
33. Johnson, S. J., Taylor, J. S., and Beese, L. S. (2003) Processive DNA synthesis observed in a polymerase crystal suggests a mechanism for the prevention of frameshift mutations, *Proc. Natl. Acad. Sci. U.S.A. 100*, 3895−3900.
34. Hogg, M., Aller, P., Konigsberg, W., Wallace, S. S., and Doublié, S. (2007) Structural and biochemical investigation of the role in proofreading of a β hairpin loop found in the exonuclease domain of a replicative DNA polymerase of the B family, *J. Biol. Chem. 282*, 1432−1444.

BI700380A